Stand-off Femtosecond Laser Induced Breakdown Spectroscopy of Metals, Soil, Plastics and Classification Studies

N. Linga Murthy, S. Abdul Salam, S. Venugopal Rao*

Advanced Center of Research in High Energy Materials **(ACRHEM)**,

University of Hyderabad, Hyderabad 500046, Telangana, India

*Corresponding author e-mail: ***soma_venu@uohyd.ac.in* OR *soma_venu@yahoo.com***

Abstract **The femtosecond stand-off laser induced breakdown spectroscopy (fs ST-LIBS) experiment is optimized for 5m distance. The fs ST-LIBS spectra of metals, alloys, soil, organic samples are recorded. Most of the atomic peaks and molecular peaks like CN, C₂, and Aluminum oxide are identified from the characteristic emission lines in the spectra. The signal to noise ratio is reduced compared to the near field case. The similarities existing in the spectral emission lines collected from different targets limits the technique for identification. We have used principal component analysis (PCA) which improves the identification and classification of the materials used as targets.**

Keywords: Fs-LIBS, Standoff, Principal Component Analysis

I. INTRODUCTION

Laser induced breakdown spectroscopy (LIBS) is a versatile technique with a potential to be deployed in hazardous environments for quick testing/analyzing various materials at a distance. LIBS has proven applications in diverse fields. Areas that benefit from LIBS include explosive detection [1, 2, 3], mining, atmosphere monitoring, and exploration of planets etc. It is based on the elemental analysis from the emission spectra of ions, atoms and molecules of the plasma. It also has the advantage of simultaneously using Raman spectroscopy and LIBS with same instrumentation, which is demonstrated in stand-off configuration by Moros et al. [4]. Both molecular and elemental information can be acquired at the same time. The signal to noise ratio can be improved by using double-pulse standoff LIBS [5, 6]. These methods can be employed for plastic waste sorting and recycling of metals in real time for environmental benefits. As the signal to noise ratio decreases with the distance in LIBS and LIBS and multivariate analysis [7] together could overcome the problem of identification as well as classification of different compounds [8, 9].

II. EXPERIMENTAL DETAILS

The 800 nm,1 kHz repetition rate and 1.8 W (average power), ~50 femtosecond pulses are focused on to the target at 6 meters using the combination of -50 cm concave and 100 cm convex lenses in Galilean configuration. The target is placed on the Newport transnational stage to move the target both in x and y plane. A Schmidt-Cassegrain telescope of 6 inches aperture placed at five meters from the target is used for collecting the characteristic optical emissions from the plasma. These emissions are fed in to a very sensitive and gated spectrograph (Mechelle spectrometer and Andor istar ICCD combination) using a 600 micron optical fiber. The setup is shown in Fig. 1. The gate delay is optimized for intense signal. The gate width is

set for 2 μs and each spectrum of a target is the integration of 2000 pulses and 40 accumulations. The wavelength range of the spectrum acquired is from 230 nm to 850 nm. 20 spectra of each target are recorded to achieve better classification. The fs LIBS spectra of all the targets used are shown in the figures 2(a)-(f).
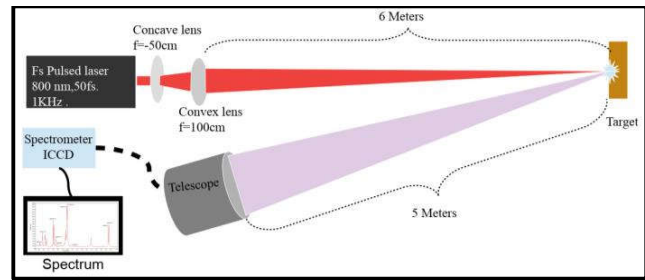

Fig. 1. *Schematic of experiment for stand-off fs-LIBS with target placed at beam 6 meters. A combination of concave and convex lenses for are used for focusing. The emissions are collected at 5 meters from the target with the telescope.*
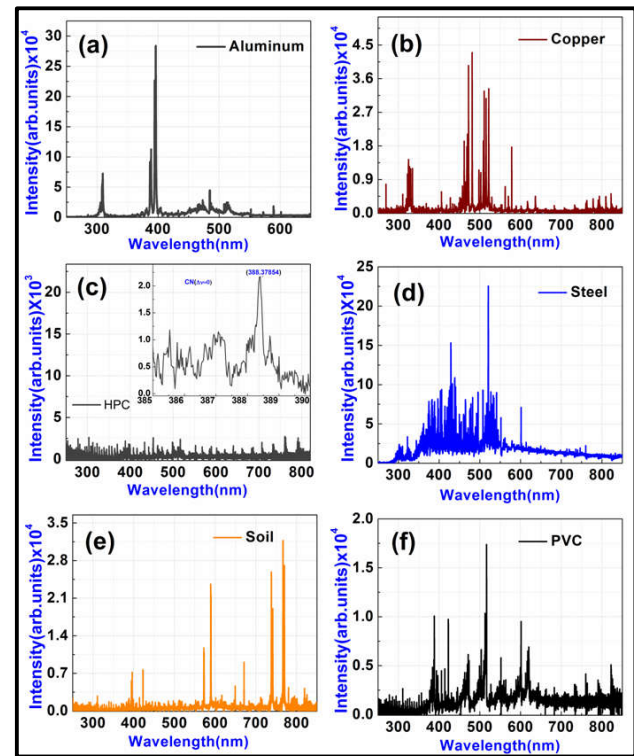

Fig. 2. *Spectra of the targets used for the experiment **(a)** aluminum **(b)** copper **(c)** HPC **(d)** steel **(e)** soil in pellet form **(f)** PVC.*

III. Results and discussions

Atomic Emissions

Aluminum atomic emissions are strong at maximum intensity at 3.0×10^5 counts compared to all the materials and HPC emission are low at intensity 2.0×10^3 counts. Manganese, chromium, iron lines are observed in steel and the same are tabulated in table I. Calcium, potassium, sodium, molybdenum, iron lines are observed in soil and are tabulated in the table II. Major copper peaks are tabulated in table III.

TABLE I. STEEL PEAKS

	Steel peaks		
Sl.no	*Observed peaks*	*reference peaks NIST*	*Ionization state*
1	344.13	344.18	Mn II
2	346.64	346.05	Mn II
3	347.64	347.38	Mn II
4	349.15	348.45	Mn II
5	349.83	349.51	Mn II
6	396.46	396.38	Cr I
7	396.68	396.95	Cr I
8	398.46	398.38	Cr I
9	399.05	399.13	Cr I
10	400.2	400.17	Cr I
11	403.16	403.26	Mn I
12	403.48	403.88	Fe I
13	405.64	405.86	Mn I
14	406.44	406	Mn I
15	408.41	408.4	Mn I
16	416.57	416.56	Cr I
17	423.62	423.67	Mn I
18	425.5	425.42	Cr I
19	427.25	427.5	Cr I
20	434.54	434.46	Cr I
21	435.27	435.18	Cr I
22	438.44	438.9	Fe I
23	460.17	460.48	Mn I
24	462.73	462.68	Mn I
25	471.2	471.09	Mn I
27	478.46	478.42	Mn I
28	482.47	482.29	Mn I
29	520.67	520.7	Cr I
30	529.93	529.78	Cr I

TABLE II. SOIL PEAKS

	Soil peaks		
Sl.no	*Observed peaks*	*Reference peaks NIST*	*Ionization state*
1	388.64	388.62	Fe I
2	393.43	393.52	Ca I
3	394.5	394.6	Ca I
4	427.23	427.17	Fe I
5	428.36	428.36	Fe I
6	430.34	430.25	Ca I
7	442.62	442.54	Ca I
8	443.6	443.49	Ca I
9	526.31	526.95	Fe I
10	572.17	572.27	Mo I
11	572.8	572.87	Mo I
12	589.13	588.99	Na I
13	589.71	589.59	Na I
14	616.35	616.21	Ca I
15	649.2	649.37	Ca I
16	649.5	649.96	Ca I
17	714.96	714.81	Ca I
18	766.7	766.48	K I
19	770.09	769.89	K I

TABLE III. COPPER PEAKS

	Copper peaks		
Sl.no	*Observed peaks*	*Reference peaks NIST*	*Ionized state*
1	510.65	510.55	Cu I
2	515.44	515.32	Cu I
3	521.89	521.84	Cu I
4	508.83	508.84	Cu II
5	502.48	502.40	Cu II

Molecular Emissions

Along with aluminum atomic transitions (tabulated in Table IV) aluminum oxide (AlO) molecular bands are also observed in fs ST-LIBS of aluminum. These AlO bands observed in range 460- 520 nm correspond to the transition $B^2\sum^+ \rightarrow X^2\sum^+$ for $\Delta\upsilon$ = -1, 0, 1 [10]. The intense peaks from each transition band are identified and shown in Fig. 3. The CN violet band [11] corresponds to the transition $B^2\sum^+ \rightarrow X^2\sum^+$ for $\Delta\upsilon$ = -1, 0, 1 are in the range 357-360 nm, 384-389 nm and 414-423 nm respectively and are observed in PVC. $\Delta\upsilon$ = 0 (peak at 388.3 nm) lines with very low intensity are observed in HPC. C_2 swan band corresponds to the transition $d^3\Pi^g \rightarrow a^3\Pi^u$ (Peaks at 471.5 nm, 516.5 nm and 563.5 nm) $\Delta\upsilon$ = -1, 0, 1 in the range 460-475 nm, 510-520 nm and 550-565 nm are observed in PVC and its intensity is greater than that of CN band. C_2 peaks are not observed in HPC. CN, C_2 peaks are tabulated in table V. The major peaks of CN, C_2 in the PVC are depicted in the Fig. 4.
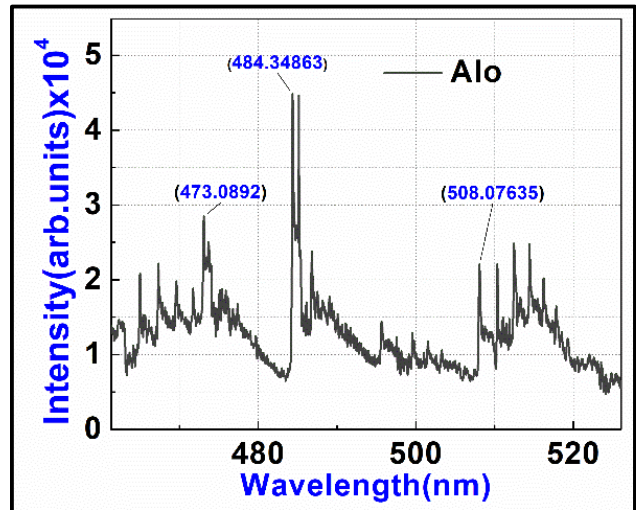

Fig. 3. *Fs LIBS spectra of Aluminum. The aluminum oxide (AlO)bands with major peaks are identified*
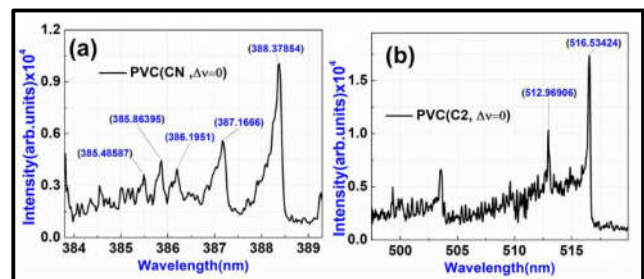

Fig. 4. *The molecular bands observed in PVC are depicted in the above figure (a) shows CN violet band and (b) shows C_2 swan band. The intense molecular peaks are identified.*

TABLE IV.   ALUMINUM PEAKS

Aluminum peaks			
Sl.no	*Observed peaks*	*Reference peaks NIST*	*Ionization state*
1	394.4	394.47	Al I
2	396.15	396.21	Al I
3	386.61	386.85	Al I
4	308.16	308.21	Al I
5	308.405	308.70	Al I
6	309.18	308.98	Al I
7	309.52	309.27	Al I

TABLE V.   PVC PEAKS

PVC Peaks			
Sl.no	*Observed peaks*	*Reference peaks NIST*	*Ionization state*
1	378.88	378.78	Fe I
2	379.86	379.95	Fe I
3	385.51	385.03	CN(4,4)
4	385.88	385.44	CN(3,3)
5	386.2	386.14	CN(2,2)
6	387.19	387.08	CN(1,1)
7	512.97	512.80	$C_2(0,0)$
8	516.57	516.42	$C_2(1,1)$
9	589.13	588.99	Na I
10	589.71	589.69	Na I

Analysis

Twenty LIBS spectra of all the six targets are recorded for the classification purpose. Fig. 5 shows the 3 component PCA. Each point in the plot corresponds to one single spectrum. PVC and HPC form distinguishable clusters along with metals and soil.
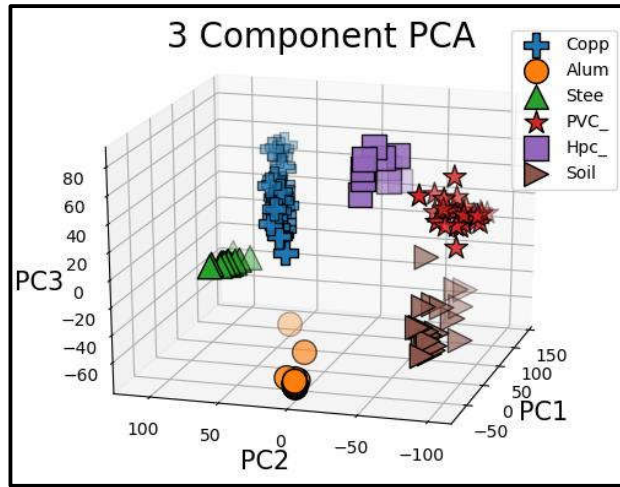

Fig. 5. *Principal component analysis of different targets. Each point in the plot corresponds to a spectrum and different shapes corresponds to different target. The distinguishable clusters demonstrate good classification.*

The major atomic and molecular peaks are identified and tabulated from the data collected in the stand-off configuration for all the targets used and a good clustering of the different targets are observed in the principal component analysis. Our future studies will be focus on the detection of trace explosives on various substrates (e.g. metal, paper, wood).

IV. CONCLUSIONS

Since the number of lenses and mirrors are more compared to near field there is considerable amount of radiation loss at each reflecting surface. The power densities at the target are reduced. The coupling of optical emissions from the target between telescope and spectrograph also contributed to losses. We have optimized the technique for the collection of emissions from various bulk targets at 5 meters and most of the peaks in the LIBS emission spectra are identified. PCA is performed on all the collected spectra and it is shown that we can achieve better classification and this technique could be used for identification/classification even when signal to noise ratio is small.

V. ACKNOWLEDGMENTS

REFERENCES

[1] Lopez-Moreno, Cristina, Santiago Palanco, J. Javier Laserna, Frank DeLucia Jr, Andrzej W. Miziolek, Jeremy Rose, Roy A. Walters, and Andrew I. Whitehouse. "Test of a stand-off laser-induced breakdown spectroscopy sensor for the detection of explosive residues on solid surfaces." *Journal of Analytical Atomic Spectrometry* 21, no. 1 (2006): 55-60.Kalam,

[2] Shaik Abdul Kalam, Nageswara Rao Epuru, Hamad Syed, Chandu Byram, and Venugopal Rao Soma. "Femtosecond laser induced breakdown spectroscopy based standoff detection of explosives and discrimination using principal component analysis." *Optics Express* 26, no. 7 (2018): 8069-8083.

[3] Kalam, Shaik Abdul, S. V. Rao, and Soma Venugopal Rao. "Standoff LIBS for explosives detection-challenges and status." *Laser Focaus World April* (2017): 24-28.

[4] Moros, Javier, Juan Antonio Lorenzo, Patricia Lucena, Luciano Miguel Tobaria, and Jose Javier Laserna. "Simultaneous Raman Spectroscopy–Laser-Induced Breakdown Spectroscopy for instant standoff analysis of explosives using a mobile integrated sensor platform." *Analytical chemistry* 82, no. 4 (2010): 1389-1400.

[5] Gottfried, Jennifer L., Frank C. De Lucia Jr, Chase A. Munson, and Andrzej W. Miziolek. "Double-pulse standoff laser-induced breakdown spectroscopy for versatile hazardous materials detection." *Spectrochimica Acta Part B: Atomic Spectroscopy*62, no. 12 (2007): 1405-1411.

[6] Xin, Yong, Lan-Xiang Sun, Zhi-Jia Yang, Peng Zeng, Zhi-Bo Cong, and Li-Feng Qi. "In situ analysis of magnesium alloy using a standoff and double-pulse laser-induced breakdown spectroscopy system." *Frontiers of Physics* 11, no. 5 (2016): 115207..

[7] Shaik Abdul Kalam, and Venugopal Rao Soma. "Discrimination of bimetallic alloy targets using femtosecond filament-induced breakdown spectroscopy in standoff mode." *Optics letters* 43, no. 15 (2018): 3465-3468.

[8] Yu, Ke-Qiang, Yan-Ru Zhao, Fei Liu, and Yong He. "Laser-induced breakdown spectroscopy coupled with multivariate chemometrics for variety discrimination of soil." *Scientific reports* 6 (2016): 27574.

[9] Unnikrishnan, V. K., et al. "Analytical predictive capabilities of laser induced breakdown spectroscopy (LIBS) with principal component analysis (PCA) for plastic classification." *Rsc Advances* 3.48 (2013): 25872-25880.

[10] Parigger, Christian G. "Atomic and molecular emissions in laser-induced breakdown spectroscopy." *Spectrochimica Acta Part B: Atomic Spectroscopy* 79 (2013): 4-16.

[11] Mousavi, S. J., M. Hemati Farsani, S. M. R. Darbani, A. Mousaviazar, M. Soltanolkotabi, and A. Eslami Majd. "CN and C 2 vibrational spectra analysis in molecular LIBS of organic materials." *Applied Physics B* 122, no. 5 (2016): 106.Mousavi, S. J. et al. "CN and C_2 vibrational spectra analysis in molecular LIBS of organic materials." *Applied Physics B* 122.5 (2016): 106.